Magnetization dynamics in La0.67Ca0.33MnO3 epitaxial films probed with resonant and non-resonant microwave absorption

Rajni Porwal, R. P. Pant, and R. C. Budhani

Citation: Journal of Applied Physics **117**, 013904 (2015); doi: 10.1063/1.4905262
View online: http://dx.doi.org/10.1063/1.4905262
View Table of Contents: http://scitation.aip.org/content/aip/journal/jap/117/1?ver=pdfcov
Published by the AIP Publishing

Magnetization dynamics in $La_{0.67}Ca_{0.33}MnO_3$ epitaxial films probed with resonant and non-resonant microwave absorption

Rajni Porwal, R. P. Pant, and R. C. Budhani[a)]
National Physical Laboratory, Council of Scientific and Industrial Research, Dr K S Krishnan Marg, New Delhi-110012, India

(Received 2 October 2014; accepted 18 December 2014; published online 5 January 2015)

Temperature (T) dependent microwave absorption measurements are performed on $La_{0.67}Ca_{0.33}MnO_3$ (LCMO) epitaxial thin films of thickness 100 and 200 nm in an electron paramagnetic resonance spectrometer operating in X-band. The resonant absorption peak is monitored for out-of-plane ($H^{\perp}$) and in-plane ($H^{\parallel}$) dc magnetic field (H) as the system goes through magnetic ordering. These data suggest a resilient transformation to the ferromagnetic (FM) phase in the vicinity of the Curie temperature (T_C), indicative of a phase separation, which is dominant in the thinner film. The saturation magnetization is calculated from SQUID magnetometry on the same film. A pronounced zero-field absorption is seen in $H^{\parallel}$ geometry displaying anomalous growth in 100 nm film at $T < T_C$. This feature is correlated with the magneto-conductivity of the manganite which is colossal in the vicinity of T_C in the well-ordered film of thickness 200 nm. Signature of standing spin wave modes is seen in $H^{\perp}$ measurements which are analyzed to calculate the spin wave stiffness constant $D(T)$ in the limit of zero temperature. The same is also inferred from the decay of equilibrium magnetization in the framework of Bloch law. These studies reveal that a bulk like LCMO is obtained in the fully relaxed thicker films. © *2015 AIP Publishing LLC*.
[http://dx.doi.org/10.1063/1.4905262]

I. INTRODUCTION

Lanthanum-based manganites with stoichiometry $La_{1-x}Ca_xMnO_3$ have attracted immense interest because of their exotic electrical and magnetic properties emanating from the coupling between the lattice, orbital, spin, and charge degrees of freedom. Depending on the value of x, the ground state of these compounds can be an antiferromagnetic Mott insulator, a metallic ferromagnet (FM) or a charge ordered (CO) insulator.[1–4] For compositions at the boundary of FM and CO phases, the $La_{1-x}Ca_xMnO_3$ can even show phase coexistence and switching from one phase to other. In thin epitaxial films, this phase duality can also be trigger by substrate induced strain.[5] During recent years, the phenomenon of magnetic phase separation near the Curie temperature (T_C) has attracted wide spread interest because of its potential application as memristor devices.[6] While several probes have been used to study phase separation in manganites, the coexisting of various ferromagnetic, paramagnetic and antiferromagnetic phases, their anisotropies and the dynamics of magnetization can be addressed in a rigorous manner using the electron spin resonance (EPR) technique.[7–13] For example, Tovstolytkin *et al.*[7] have used EPR to investigate the complex phase separation in $La_{0.6}Ca_{0.4}MnO_3$ films grown on $NdGdO_3$ (001) under specific condition. Here, the EPR technique established coexistence of two ferromagnetic phases of widely differing T_C. The intrinsic magneto-resistance (MR) in $La_{0.7}Ca_{0.3}MnO_3$ films and its dependence on the angle between magnetic field and crystallographic axis have been studied by Golosovsky *et al.*[8] Since in many potential applications the manganites would be used in a thin film form, it is important to establish how the relative phase content and thus the electro-magnetic response will be affected by film thickness, choice of the substrate and growth temperature. Even though quite a few studies have been carried out to explore the magnetic properties of manganites using FMR, a comparison of how FMR and EPR spectra evolve as a function of film thickness and magnetic field orientation still need to be addressed. In view of this, we have carried out both temperature and angle dependent studies of FMR on Pulsed laser deposited LCMO thin epitaxial films using resonant and non-resonant microwave absorption. These studies have allowed us establish magnetic phase separation, non-resonant absorption due to eddy currents and measurement magnetization $M(T)$. We have also measured the static spin wave modes and from their magnetic field and temperature dependence inferred the spin wave stiffness constant. Further, the Bloch law for suppression of saturation magnetization by spin wave excitation H applied to deduce the stiffness constant.

II. EXPERIMENT

The epitaxial thin films of $La_{0.67}Ca_{0.33}MnO_3$ of thickness 100 and 200 nm were deposited on (001) oriented $SrTiO_3$ substrates using KrF excimer ($\lambda = 248$ nm) laser based pulsed laser deposition technique.[14] The stoichiometric target used for deposition was prepared through solid state reaction route. In order to attain high quality epitaxial thin films, the deposition temperature was kept at 800 °C and the films were grown at a slow (<1 Å/s) rate. The oxygen stoichiometry of the film was optimized by post deposition annealing at 500 °C for 30 min in oxygen atmosphere. The basic structural and electrical characterization of the films was carried out with θ-2θ X-ray

a)Author to whom correspondence should be addressed. Electronic mail: rcb@iitk.ac.in.

diffraction and four probe resistivity measurements down to 5 K, respectively. The magnetic ordering temperature and magnetization measurements were performed using a Quantum Design make superconducting quantum interference device (SQUID) magnetometer. To investigate anisotropy profiles, coercive field (H_c), MR and magnetic phase separation, we have performed FMR measurements in the temperature range of 300–120 K using Bruker Biospin A 300 EPR spectrometer operating in the "X"- band (9.5 GHz). In order to keep the Q-factor of the cavity to a reasonable value, samples were cut into small $1 \times 1\,mm^2$ pieces. All FMR measurements were carried out with modulation amplitude of 10 Oe and modulation frequency of 100 kHz. For the precise alignment of external field in the plane of the film, angle dependent measurements of the resonance field were carried out and then the sample was locked at the angular position where the resonance field was minimum.

III. RESULTS AND DISCUSSION

A. Crystallographic structure and magnetic ordering

We first discuss the crystallographic structure of the $La_{0.67}Ca_{0.33}MnO_3$ (LCMO) films. Figure 1(a) shows the θ-2θ X-ray diffraction pattern of the films of thickness (d) of 100 and 200 nm. In the bulk form, $La_{0.67}Ca_{0.33}MnO_3$ is cubic (a = 0.386 nm). A shift in LCMO diffraction peaks towards higher 2θ value on the reduction of thickness has been observed which corresponds to a change in the out-of-plane lattice parameter from c ≈ 0.3817 nm (for d = 200 nm) to c ≈ 0.3805 nm (for d = 100 nm). This shift is shown in inset of Fig. 1. The decrease in "c" parameter can be well understood in view of epitaxial tensile strain in the a-b plane due to ≈1% higher lattice parameter of $SrTiO_3$. This a-b plane strain in $La_{0.67}Ca_{0.33}MnO_3$ film decreases gradually on increasing the thickness.

In Fig. 2, we have plotted the resistivity of the two LCMO films over a temperature range of 5–300 K. Consistent with

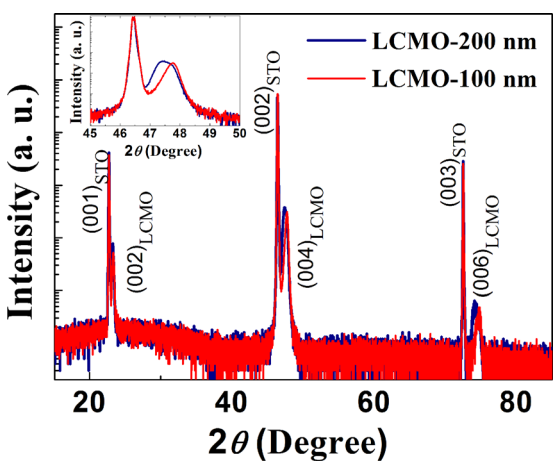

FIG. 1. X-ray θ-2θ diffraction pattern of $La_{0.67}Ca_{0.33}MnO_3$ films of thickness 100 and 200 nm in the vicinity of the (002), (004) and (006) reflections of the $SrTiO_3$ substrate. The inset highlights the shift of (004) reflection for two different thickness of the film. The diffraction profile was acquired using a CuK_α source.

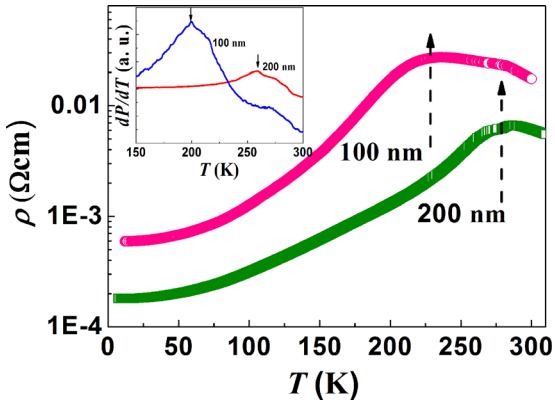

FIG. 2. Electrical resistivity of the LCMO films deposited on $SrTiO_3$. The measurement has been carried out in the temperature range of 10 K to 300 K. Inset shows dP/dT from 100 K to 300 K. The Curie temperature is marked with arrows.

earlier studies,[15] the resistivity initially increases on lowering the temperature below 300 K. This semiconducting behavior is a characteristic feature of the paramagnetic state in LCMO. In $La_{0.67}Sr_{0.33}MnO_3$ on the other hand, the paramagnetic state is metallic.[16] The resistivity reaches a peak value and then drops continuously down to the lowest temperature of measurement (5 K), marking a metallic behavior. The temperature at which the resistivity reaches the peak value below 300 K corresponds to the Curie temperature (T_C) of the material. The T_C of 100 and 200 nm thick films in this case is ≈235 and ≈275 K, respectively. We note that the T_C of the thicker film is same as the Curie temperature of $La_{0.67}Ca_{0.33}MnO_3$ bulk crystals.[17] Earlier studies on LCMO epitaxial films have shown a gradual reduction in T_C on decreasing the film thickness.[18] Our data on the 100 nm thick film are consistent with this observation.

B. Resonant microwave absorption

We now present the microwave absorption spectra of the 200 nm thick LCMO film. Figures 3(a) and 3(c) show the differential absorption (dP/dH) measured in X-band at several temperatures from 150 K to 300 K in a configuration where the dc magnetic field was out of the plane of the film [Fig. 3(a)] and in the plane [Fig. 3(c)]. A distinct resonant absorption is seen at 300 K in both the geometries and its position in field is the same (≈3400 Oe). On cooling the sample down to 280 K, the position of the resonance peak remains fixed. However, below this temperature, significant changes in the shape and position of the absorption profile are seen. From the resistivity and dc magnetization measurements, it is noted that the magnetic ordering temperature of the sample is ≈275 K. The sharp absorption seen down to 280 K can therefore be attributed to the paramagnetic resonance of the uncorrelated spins at different Mn^{3+} and Mn^{4+} sites in the sample. The frequency ω of the resonance signal is related to field (H_r^{PM}) as,

$$\omega = \gamma H_r^{PM}, \quad (1)$$

where γ and H_r^{PM} are the gyromagnetic ratio and resonance field, respectively.

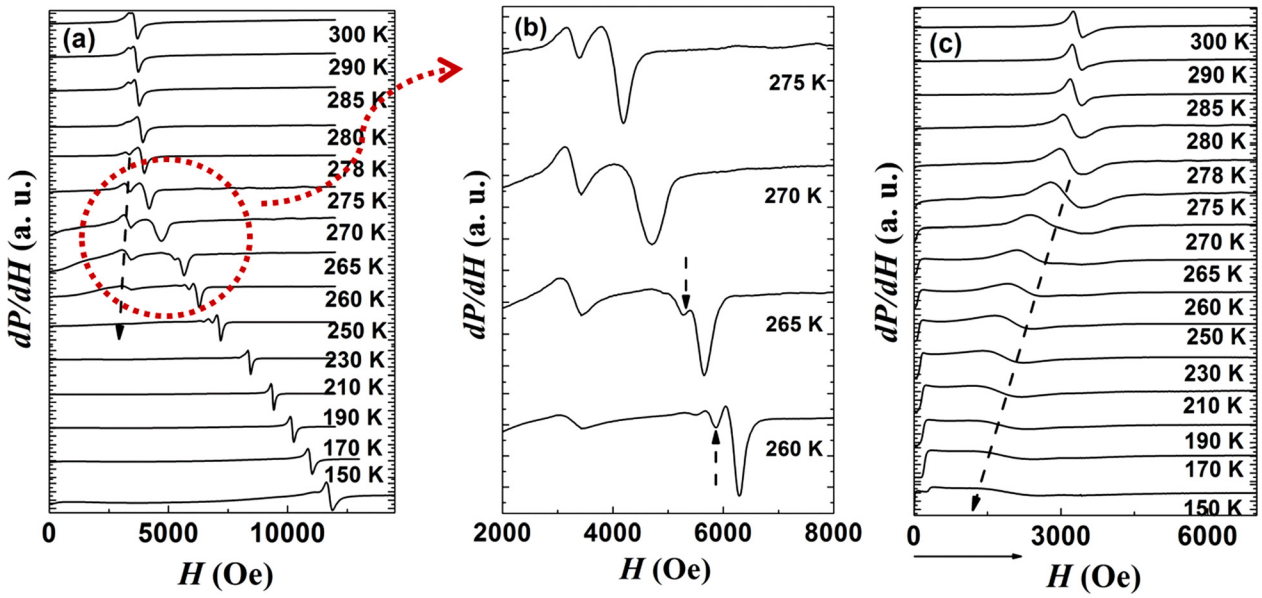

FIG. 3. Differential absorption dP/dH vs H of LCMO 200 nm thin film at temperature 150–300 K for field applied (a) out-of-plane and (c) in-plane to the film plane. The arrow at the bottom shows the direction of the field sweep. Dashed line indicates the change in Hr with temperature. (b) View of expanded spectra of (a) in the temperature range 275–260 K. Here, phase transformation can be clearly seen and the small satellite peaks are spin wave modes.

However, once the spins start to order, the resonance fields for parallel ($H_r^{\parallel}$) and perpendicular ($H_r^{\perp}$) geometries are expressed as,

$$\omega = \gamma[H_r^{\parallel}(H_r^{\parallel} + 4\pi M)]^{\frac{1}{2}}, \tag{2}$$

$$\omega = \gamma(H_r^{\perp} - 4\pi M), \tag{3}$$

respectively.[9,10] Since the frequency is fixed and magnetization M grows on lowering the temperature below T_C, it is clear from these relations that $H_r^{\parallel} < H_r^{PM}$ and $H_r^{\perp} > H_r^{PM}$. Further, these inequalities grow on lowering the temperature. The general trend of the resonance line seen in Figs. 3(a) and 3(c) is consistent with these inferences. Interestingly, however, the spectrum itself for $H^{\perp}$ configuration [Fig. 3(a)] is quite rich in the temperature range 275 to 260 K. In Fig. 3(b), we have plotted an expanded version of these spectra. Here, the main FMR peak shifts to higher field on lowering the temperature. This resonance also has a satellite structure which appears prominently between 260 and 250 K. But more importantly, a feature similar to the line in the paramagnetic phase remains down to 250 K, albeit with much reduced intensity. The contour of this peak is shown by the dotted line in Fig. 3(a). This observation is an indication of a phase separation in the material, where the remaining paramagnetic phase undergoes ordering at a lower temperature.

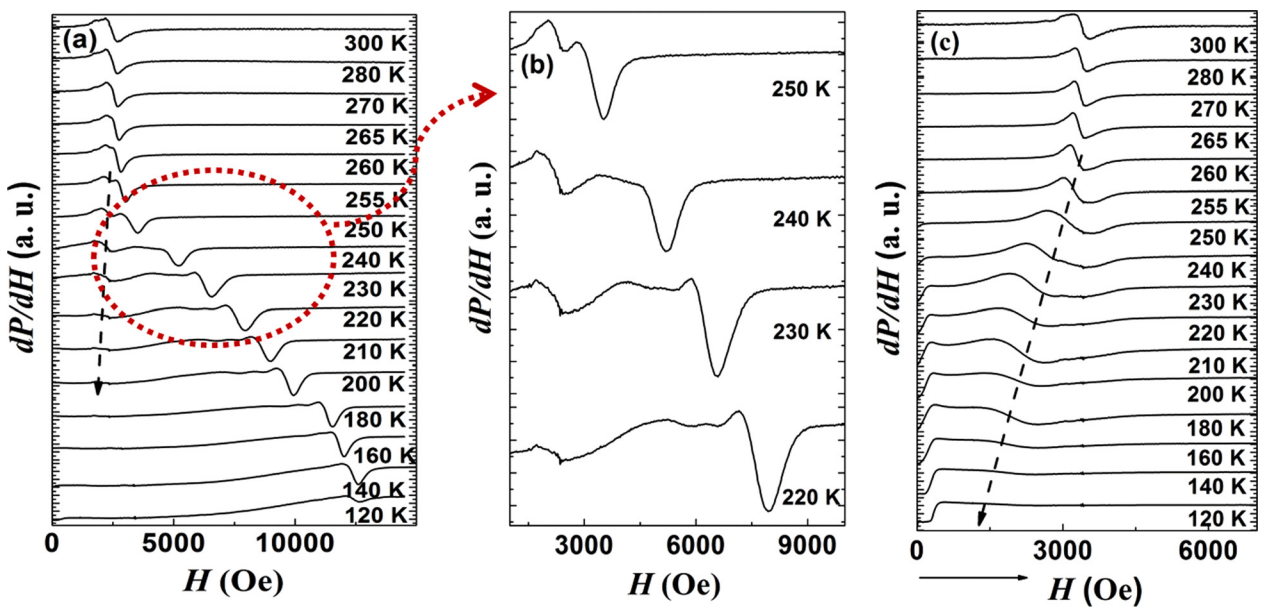

FIG. 4. Differential absorption dP/dH vs H of LCMO 100 nm thin film at temperature 120–300 K for field applied (a) out-of-plane and (c) in-plane to the film plane. The arrow at the bottom shows the direction of the field sweep. Dashed line indicates the change in Hr with temperature. (b) View of expanded spectra of (a) in the temperature range 250–220 K. Here, phase transformation can be clearly seen and the small satellite peaks are spin wave modes.

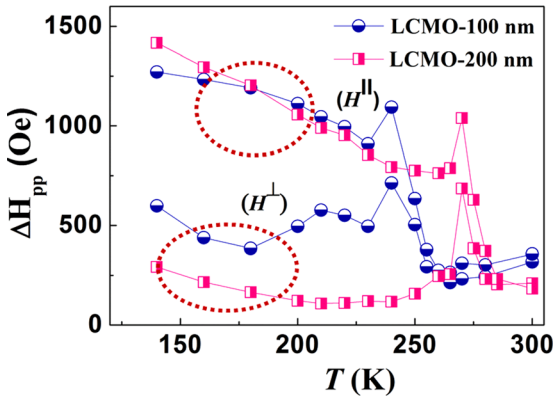

FIG. 5. Variation of peak-to-peak line width (ΔH_{pp}) with temperature for LCMO 100 and 200 nm thick films in parallel and perpendicular fields.

The satellite structure shown by dotted arrow in Fig. 3(b) appears to be the contribution of spin-wave resonance (SWR) in the perpendicular field geometry. Figure 3(c) shows the evolution of the FMR derivative absorption for the d = 200 nm film when the dc field was in the plane of the film. For the TE 102 cavity used here, the RF field is also in the plane of the film but orthogonal to the dc field. The FMR peak for $H_r^{\parallel}$ geometry becomes feeble below ≈190 K. In this geometry, we also see a large zero-field absorption which will be discussed in the subsequent section. The derivative absorption (dP/dH) of the 100 nm film for out-of-plane and in-plane magnetic field is shown in Figs. 4(a)–4(c). The general features of the absorption spectra are same as in Figs. 3(a)–3(c), but the critical features marking PM to FM transition appear at a lower temperature.

The width of the FMR line of a ferromagnetic film and its dependence on the angle between field direction and film plane provide information about magnetic inhomogeneties in the sample.[11] In Fig. 5, we compare the line width (ΔH_{pp}) of the 100 and 200 nm LCMO films for measurements in $H_r^{\parallel}$ and $H_r^{\perp}$ geometries. The line width in the paramagnetic state is only ≈250 Oe. At the magnetic transition, we see a jump in ΔH_{pp} in the vicinity of the T_C followed by a nearly monotonic growth down to the lowest temperature of measurement, where it is ≈1.5 kOe. It is interesting to note that at $T > T_C$ the ΔH_{pp} of both the films is nearly the same. While for a soft magnetic film the line width is expected to be constant in temperature, the observed temperature dependence is common in all epitaxial manganite films grown at moderate temperatures (800 ∼ 850 °C).[9] High temperature (≈1000 °C) annealing can perhaps lead to a much more homogeneous magnetic state.[11] Figure 5 also shows the resonance line width for $H_r^{\perp}$ geometry. We note a small and nearly field independent line width for $T < T_C$ for the 200 nm film, while for the 100 nm film, it is significantly larger. This suggests some in-plane magnetic disorder in these films.

In Fig. 6(a), we show the behaviour of $H_r^{\perp}$ and $H_r^{\parallel}$ for the two films as a function of temperature. The two critical fields in the paramagnetic state are the same. The splitting of the single curve below T_C and their subsequent behaviour at still lower temperatures is due to the growth of ordered magnetic

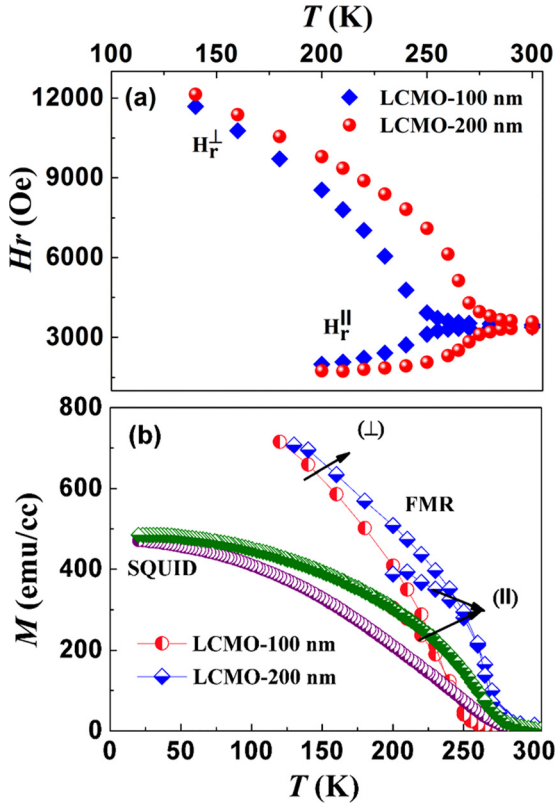

FIG. 6. (a) Variation of the resonance field as a function of temperature for 100 and 200 nm thick $La_{0.67}Ca_{0.33}MnO_3$ films. We note that $H_r^{\perp}$ increases while $H_r^{\parallel}$ drops on lowering on temperature. The resonance peak for $H^{\parallel}$ geometry becomes extremely feeble below ≃150 K. The magnetization M(T) calculated making use of the Kittel Eqs. (2) and (3) is plotted in Fig. 6. (b) The difference between the magnetization arises as in FMR, anisotropy term is also included.

moment M(T). The intensity of the resonant absorption in $H^{\parallel}$ geometry drops significantly below ∼190 K and the identification of H_r below this temperature has large uncertainty. Making use of Eq. (3), we have calculated the saturation magnetization [M(T)] of the two films in the $H^{\parallel}$ and $H^{\perp}$ geometries. However, for $H^{\parallel}$ the calculation is limited to $T \geq 200$ K. These data are compared with the results of SQUID measurements on the same samples in the parallel field geometry at 8000 Oe. The high field has been used to ensure saturation of magnetization. These data have been corrected for the diamagnetic contribution of the substrate. We notice a reasonable agreement between the SQUID results and $H^{\parallel}$ measurement. It is worthwhile to mention that the M(T) of 100 nm film measured in the SQUID magnetometer shows anomalous temperature dependence in the temperature window of ∼150 to 220 K, suggesting inhomogeneties in the sample.

C. Non-Resonant microwave absorption

One interesting feature of the parallel field data shown in Figs. 3(c) and 4(c) is a distinct jump in the baseline for dP/dH at zero-field. This feature emerges below T_C and as the field goes from $H^{\parallel}$ to $H^{\perp}$ Configuration, the abrupt change in dP/dH for $H^{\parallel}$ translates T_C in to a gradually increasing slope of the base line. These features are

intimately linked with the eddy current losses in the manganite[12] and can be expressed in terms of the imaginary part of the microwave magnetic susceptibility[8]

$$\chi'' = \frac{\mu_0 \omega \sigma d^2}{12}, \tag{4}$$

where σ and d are the electrical conductivity and thickness of the film, respectively. The manganites like $La_{0.70}Ca_{0.30}MnO_3$ show a colossal negative magnetoresistance effect due to double exchange mechanism between Mn^{3+} and Mn^{4+} ions through the bridging oxygen, which also facilitates ferromagnetic ordering. It has been shown earlier by Golosovsky *et al.*[8] that the change in conductivity due to CMR effect can be expressed as;

$$\Delta\sigma^{CMR} = \sigma(H) - \sigma(0) \approx \chi_0 \frac{d\sigma}{dM}\left[H\cos(\theta - \psi) - H_a \cos^2\theta\right]. \tag{5}$$

This expression assumes easy plane anisotropy, with anisotropy field H_a. The angles ψ and θ define the directions of external dc field ($\vec{H}$) and the magnetization $\vec{M}$ with respect to sample normal, respectively, and $\chi_0 = dM/dH$. With the use of Eqs. (4) and (5) and a few more steps of algebra, it can be shown[8] that the derivative of the absorbed power (dP/dH) is proportional to $d\sigma/dM$ and hence a measure of the CMR effect ($\Delta\sigma^{CMR}$).

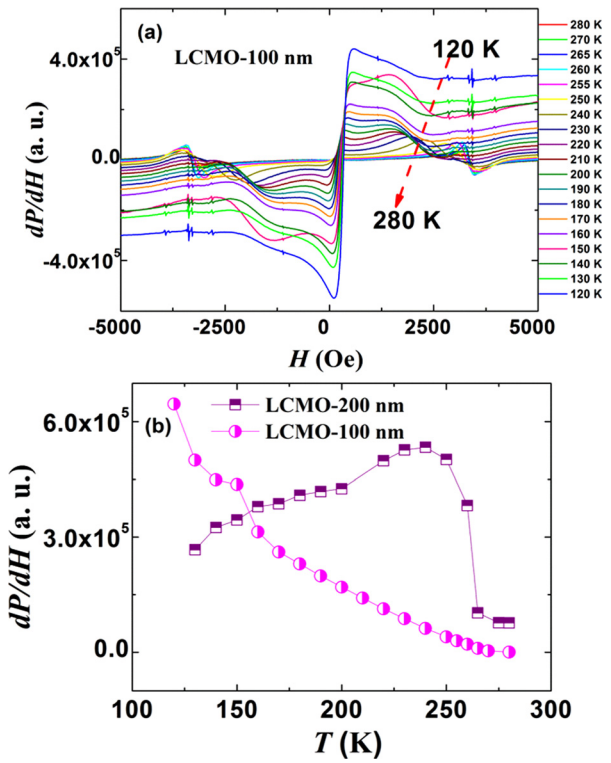

FIG. 7. (a) Absorption derivative at different temperatures from 120 K–280 K for LCMO 100 nm film in-plane orientation. Here, direction of the field sweep is from $H = -5$ kOe to $+5$ kOe. Phase transition in LCMO film leads to the discontinuity in the base line originates from microwave magnetoresistance. (b) Temperature dependence of the magnetoresistance at $H = 10$ kOe for LCMO 100 and 200 nm thick films.

In Fig. 7(a), we show the zero-field anomaly in dP/dH for the 100 nm film in $H^{\parallel}$ geometry. When the field is swept in both directions near H = 0 we also see a narrow hysteresis. The important point to note in Fig. 7(a) is a superlinear growth of the zero-field step on lowering the temperature. Such a growth is not observed in the 200 nm thick film. In Fig. 7(b), we plot the difference in dP/dH base line at ± 1 Tesla for the two films in $H^{\parallel}$ geometry. It is interesting to note that the non-resonant absorption for the 200 nm film peaks in the vicinity of the Curie temperature. This behaviour is consistent with the results of magnetoresistance measurements in epitaxial films of manganites.[8] However, as the film thickness reduces, the magnetic transition temperature goes down and the ordered moment grows gradually on lowering the temperature as seen in Fig. 6(b). Since magnetic ordering and conductivity are intimately linked in double exchange ferromagnets, the gradual rise of dP/dH on lowering the temperature as seen in Fig. 7(b) for the 100 nm film can be attributed to non-saturation of magnetic moment.

D. Spin wave mode analysis

As shown by Kittel,[19] standing spin wave resonance (SWR) modes can be excited in a ferromagnetic thin film placed in a perpendicular magnetic field because of surface pinning of moments or due to magnetic inhomogeneties in the interior of the film. Studies of the temperature dependence of such modes give valuable information about the exchange interaction J which makes the spins order. For a film with easy plane anisotropy, SWR modes are excited when the microwave magnetic field h_{mw} is perpendicular to the dc magnetic field. As shown in Ref. 13, for dc field aligned parallel to film normal, the spin wave modes are given by;

$$H_n - H_0 = H_a - \frac{\pi n^2}{\gamma d^2} D, \tag{6}$$

where n is an integer and H_n correspond to the spin wave resonance fields of mode n. The other parameters of Eq. (6) are the FMR field $H_0 (= \frac{\omega}{\gamma})$, spin wave stiffness constant D and γ the gyromagnetic ratio.

The stiffness constant in turn is related to the exchange integral J as, $D = \frac{2Jsa^2}{\hbar}$, where s and a are the site spin and lattice constant of the spin lattice. From Eq. (6), it is clear that a plot of H_n vs n^2 would yield information about D and the anisotropy field H_a. Figure 8(a) shows the perpendicular field resonance and its higher harmonics for the 200 nm thick film. A zoomed version of dP/dH is also shown and odd number modes up to n = 9 can be located in the absorption spectrum. The odd number assignment has been done on the basis of least squares fit to H_n vs n^2, assuming that the strongest peak corresponds to n = 1 [see Fig. 8(b)]. The intensity of modes varies approximately as $1/n^2$ as shown in the inset of Fig. 8(b). These intensities are generally functions of metallicity of the samples and measurement frequency.[20,21] From the H_n vs n^2 plots at several temperatures, we have extracted the spin wave stiffness constant $D(T)$, which for the 200 nm thick film at a reduced temperature (T/T_C) of 0.9 and 0.8 is 70 and

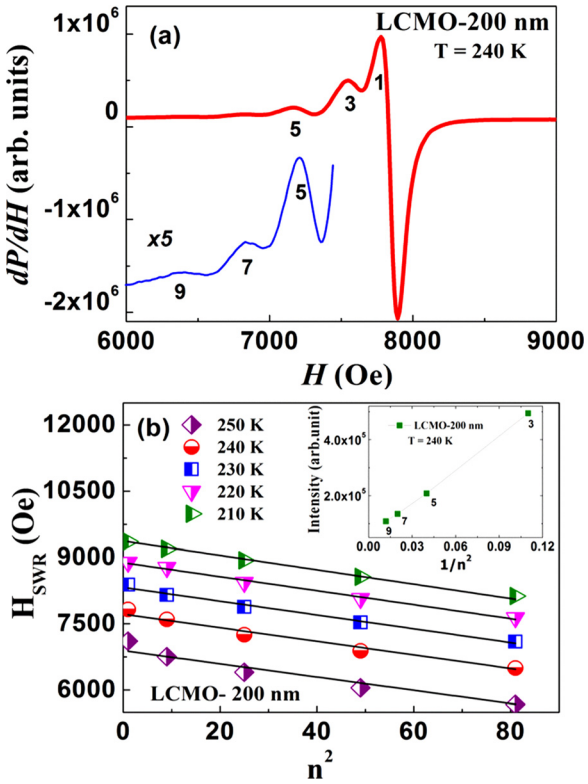

FIG. 8. (a) Spin-wave resonance spectrum for LCMO-200 nm film at 240 K in the perpendicular magnetic field. The mode number is marked at on peak. The inset shows the 5–9 SWR modes zoomed out by a factor of five. (b) Plot of SWR modes at different temperature for LCMO-200 nm film for the perpendicular field configuration. The solid lines show the linear fit to the data. The inset shows the intensity of spin-wave modes vs mode number dependence.

76 meVÅ^2, respectively. For the 100 nm film the D at these reduced temperatures is ≈51 and ≈74 meVÅ^2. These numbers are in the same range as reported for $La_{0.7}Ca_{0.3}MnO_3$ (Ref. 13) and $La_{0.67}Ba_{0.33}MnO_3$ films.[22] The temperature dependence of $D(T)$ over a limited range of temperature is shown in Fig. 9. The $T^{5/2}$ dependence seen here is consistent with the theory.[22,23] From these data, we extract a $D(0)$ of ≈128 meVÅ^2 and 87 meVÅ^2 for the 100 and 200 nm thick films, respectively. At this stage, it may be worthwhile to extract spin wave stiffness constant from the temperature dependence of magnetization at $T/T_C \ll 1$. In metallic ferromagnets, the magnetization drops much faster with temperature as compared to the mean-field behaviour of $M_s(T)/M_s(0)$. As per Bloch law, the suppression of magnetization goes as $M_s(T)/M_s(0) \sim 1\text{-}AT^{3/2}$. In the inset of Fig. 9, we plot M(T)/M(0) for $T/T_C \leq 0.2$. Solid lines in the figure show fit to the Bloch behaviour. The coefficient "A" extracted from these fits is $\sim 1.04 \times 10^{-4} K^{-3/2}$ and $2.50 \times 10^{-5} K^{-3/2}$ for the 100 and 200 nm thick films, respectively. The Bloch law, however is valid strictly in the limit of zero field.[24] The coefficient A then can be related to $D(0)$ as $D(0) = (\frac{k_B}{4\pi})(\frac{g\mu_B}{M(0)A})^{2/3}$, which yield $D(0) = 37$ and 91 meVÅ^2 for the 100 and 200 nm film, respectively. These numbers are in reasonable agreement with FMR measurements.

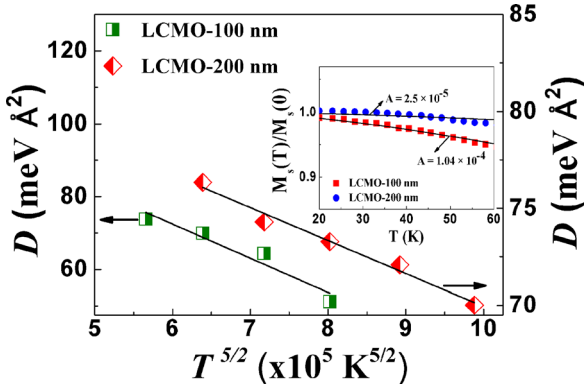

FIG. 9. The temperature dependence of the spin-wave stiffness coefficient (D) for LCMO-100 and 200 nm films. Inset is the magnetization data from SQUID which compares with the predictions of the Bloch rule.

IV. SUMMARY

We have studied the crystallographic structure, equilibrium magnetization and magnetic field dependent microwave absorption in epitaxial films of $La_{0.67}Ca_{0.33}MnO_3$ grown on (100) $SrTiO_3$. The c-axis lattice parameter measurements indicate that the thinner (100 nm) film is under in-plane tensile strain, which reflects itself in T_C, M(T) and zero-field microwave absorption. The resonant and zero-field microwave absorption for out-of-plane and in-plane dc fields have been carried out to deduce saturation magnetization, magnetoresistance, and spin wave stiffness constant. This comparative study of 100 and 200 nm thick films suggests that a bulk like behaviour of the manganite LCMO is seen in the thicker film.

ACKNOWLEDGMENTS

Rajni Porwal acknowledges the financial support from the Indo-French project (Grant No. GAP 123132) and the Department of Science and Technology, India (Grant No. GAP123532). R.C.B. acknowledges the J C Bose National Fellowship of the Department of Science and Technology, India. We thank Dr. Anurag Gupta for SQUID measurements and Dr. M. Golosovsky for helpful discussion.

[1]A. P. Ramirez, J. Phys. Condens. Mater. **9**, 8171 (1997).
[2]E. Dagotto, T. Hotta, and A. Moreo, Phys. Rep. **344**, 1 (2001).
[3]M. B. Salamon and M. Jaime, Rev. Mod. Phys. **73**, 583 (2001).
[4]M. Imada, A. Fujimori, and Y. Tokura, Rev. Mod. Phys. **70**, 1039 (1998).
[5]S. Srivastava, N. K. Pandey, P. Padhan, and R. C. Budhani, Phys. Rev. B **62**, 13868 (2000).
[6]C. Israel, M. J. Calderón, and N. D. Mathur, Mater. Today **10**, 24 (2007).
[7]A. I. Tovstolytkin, V. V. Dzyublyuk, D. I. Podyalovskii, X. Moya, C. Israel, D. Sánchez, and N. D. Mathur, Phys. Rev. B **83**, 184404 (2011).
[8]M. Golosovsky, P. Monod, P. K. Muduli, R. C. Budhani, L. Mechin, and P. Perna, Phys. Rev. B **76**, 184414 (2007).
[9]S. E. Lofland, S. M. Bhagat, H. L. Ju, G. C. Xiong, T. Venkatesan, R. L. Greene, and S. Tyagi, J. Appl. Phys. **79**, 5166 (1996).
[10]O. Arnache, P. Monod, N. Bontemps, D. Giratá, and P. Prieto, Phys. B: Condens. Mater. **384**, 71 (2006).
[11]S. E. Lofland, S. M. Bhagat, H. L. Ju, G. C. Xiong, T. Venkatesan, and R. L. Greene, Phys. Rev. B **52**, 15058 (1995).
[12]D. L. Lyfar, S. M. Ryabchenko, V. N. Krivoruchko, S. I. Khartsev, and A. M. Grishin, Phys. Rev. B **69**, 100409(R) (2004).
[13]M. Golosovsky, P. Monod, P. K. Muduli, and R. C. Budhani, Phys. Rev. B **76**, 184413 (2007).

[14]P. Padhan, W. Prellier, Ch. Simon, and R. C. Budhani, Phys. Rev. B **70**, 134403 (2004).
[15]P. Padhan and R. C. Budhani, Phys. Rev. B **67**, 024414 (2003).
[16]K. Senapati and R. C. Budhani, Phys. Rev. B **71**, 224507 (2005).
[17]D. C. Worledge, G. J. Snyder, M. R. Beasley, T. H. Geballe, R. Hiskes, and S. Di Carolis, J. Appl. Phys. **80**, 5158 (1996).
[18]V. Peña, Z. Sefrioui, D. Arias, C. León, J. Santamaria, M. Varela, S. J. Pennycook, M. Garcia-Hernandez, and J. L. Martinez, J. Phys. Chem. Solids **67**, 472 (2006).
[19]C. Kittel, Phys. Rev. **110**, 1295 (1958).
[20]R. Weber, P. E. Tannenwald, and C. H. Bajorek, Appl. Phys. Lett. **16**, 35 (1970).
[21]G. C. Bailey and C. Vittoria, Phys. Rev. Lett. **28**, 100 (1972).
[22]S. E. Lofland, S. M. Bhagat, C. Kwon, M. C. Robson, R. P. Sharma, R. Ramesh, and T. Venkatesan, Phys. Lett. A **209**, 246 (1995).
[23]F. J. Dyson, Phys. Rev. **102**, 1217 (1956); **102**, 1230 (1956).
[24]V. N. Smolyaninova, J. J. Hamilton, R. L. Greene, Y. M. Mukovskii, S. G. Karabashev, and A. M. Balbashov, Phys. Rev. B **55**, 5640 (1997).